Limit states of a stress-strain pipeline

Viktor A. Rukavishnikov[a], Oleg P. Tkachenko[a]

[a]*Computing Center of the Far Eastern Branch of the Russian Academy of Sciences, Kim Yu Chen Str., 65, Khabarovsk, 680000, Russia*

Abstract
Mathematical model of the pipeline as an elastic shell was developed. Two limiting cases of pipeline geometry were considered. An analysis was given of the fundamental differences between their stress-strain state. A numerical analysis of the deformations of a weakly bent pipeline and a pipeline with a singularity was performed. It was established that the approximate mathematical model of the weakly bent pipeline describes the original problem with high accuracy. The existence of a stress field singularity in the mathematical model of the pipeline with a kink was established.

Keywords
bent pipeline, shells, singularities, stress-strain state, numerical experiment

1. Introduction

Presently, due to the depletion of hydrocarbons in their traditional production regions, the society has begun to work on the development of oil fields in remote areas. This development involves a series of scientific problems related to the transportation of oil products to areas of their consumption. Because of the novelty and complexity, many of these problems remain unsolved, and the traditional approaches are inefficient for their solutions.

One of the unsolved issues is the problem of the pipeline deviation from its design position, appear because of the motions of soil, seismic activity, intrinsic instability, and for other reasons [1]. In this regard, the question arises concerning the study of the pipeline dynamics in a deformable medium.

On the other hand, the pipeline transport structure is very complex and subject to heavy loads [2]. As a rule, this structure contains a large number of pipes joints. One of the first problems of the correct superposition of conjugation conditions on the junction line was investigated in book [3]. Ibid was established that the task of formulating the correct conjugation conditions on the singularity lines of the shells is not trivial, and asymptotic methods were developed to solve it.

Thus, there are two limit pipeline geometries:

1. The pipe centerline curvature is small;
2. The pipe centerline curvature tends to infinity.

The aim of this work is a numerical study of the features of the stress-strain state of the pipeline at these limiting geometries.

Research objectives

1. Determination of a numerical criterion for identifying limiting cases.
2. Construction of two mathematical models of pipelines for limiting cases.

CEUR Workshop Proceedings (CEUR-WS.org)

3. Proposal of numerical analysis methods for setting up computational experiments.

4. Numerical study of the main characteristics of the stress-strain state for two limiting cases of pipe geometry.

2. Problem formulation

2.1. General geometry of the mechanical system

We refer to Figures of articles [4, 5] in the statement part of the paper.

The pipeline of length L with a circular cross-section of radius R_0 and a wall of thickness h is considered (see Figure 1 in [4]). The centerline of the pipe is curved along flat curve $\Gamma_0 = \{x_0, y_0 : x_0 = x_0(s), y_0 = y_0(s)\}$, where s is an arc length (natural parameter). The pipe is filled with a steady fluid flow, which is moving with velocity ϑ_{s0} under the influence of a constant pressure drop.

We define the curvature parameter

$$\lambda = R_0 \max |\kappa_0(s)|, \tag{1}$$

where $\kappa_0(s)$ is the initial curvature of the line Γ.

Suppose that the basic geometric relation of the theory of elastic cylindrical shells is satisfied:

$$h/R_0 \ll 1.$$

This paper assumes $h/R_0 \leq 10$; the admissibility of this is indicated in [6].

Parameter (1) allows distinguishing two limiting cases of pipe geometry:

1. $\lambda \ll 1$ — weakly bent pipe;
2. $\lambda \to \infty$ — kinked pipe.

These two cases must be investigated from two different perspectives. Approach for Case 1: the pipe is investigated as a technical Vlasov shell (see [7]). Approach for Case 2: the pipe is investigated as a moment shell (see [3]).

2.1.1. Slightly bent pipe geometry

The geometry of Case 1 was studied in detail in [8, 4].

We introduce the following curvilinear orthogonal coordinates: s is the distance along the pipe centerline and θ and R are the angle and radius of polar coordinates in the cross section at point s, see Figure 1 in [4]. The Cartesian coordinates of the pipe point are given by

$$X = x(s) + \frac{dy(s)}{ds} R \sin \theta,$$

$$Y = y(s) - \frac{dx(s)}{ds} R \sin \theta,$$

$$Z = R \cos \theta.$$

Following [9], from these formulas we can determine the components of the metric tensor, the Christoffel symbols, and the Lamé coefficients for the orthogonal coordinate system constructed.

For the middle surface of the pipe's wall, the following geometric relationships are executed:

$$A = 1 + R_0 \kappa(s, t) \sin \theta, \quad B = R_0,$$

$$k_1 = \kappa(s, t) \sin \theta \Big/ (1 + \kappa(s, t) R_0 \sin \theta), \quad k_2 = 1 \big/ R_0; \tag{2}$$

where k_1 and k_2 are the main curvatures of a median surface, κ is the axis curvature. Lame coefficients are expressed by the formulas:

$$H_1 = A(1 + k_1 \gamma), \quad H_2 = B(1 + k_2 \gamma), \quad \gamma = R - R_0. \tag{3}$$

2.1.2. Kinked pipe geometry

We will consider Case 2 by the example of two cylindrical pipes connected at right angles. Both pipes have the same radii and wall thickness. The geometry of this system was studied in [5] (see Figures 1, 2 in [5]).
We denote:
h — pipe wall thickness; R_i — inner radius of the pipe; R_e — outer radius of the pipe; L_1, L_2 — lengths of the first and second pipe sections along the centerline, respectively; $R_0 = 0.5(R_e + R_i)$ — radius of the middle surface of the pipe; $\mathcal{L}$ — line of intersection of the middle surfaces of two pipes.
   Connected pipes are referred to below as segments ① and ②.
   Let's introduce the Cartesian coordinates $(O; x, y, z)$, the point O coincides with the beginning of the first pipe. The (Ox) axis coincides with the generatrix of the segment ①. Equation of the segment ② centerline obviously is $x = L_1$. Obviously, in Cartesian coordinates, the equation of the plane of intersection of segments is:

$$x + y - L_1 = 0. \tag{4}$$

   From (4) and the formulas for the connection of cylindrical and Cartesian coordinates [10], we obtain the following geometric relations.
   Relationship formulas for Cartesian and cylindrical coordinates.
Segment ①:

$$x = s_1, \quad y = -\rho_1 \sin \theta_1, \quad z = \rho_1 \cos \theta_1; \quad x \le L_1 - y, \quad s_1 \le L_1 + \rho_1 \sin \theta_1. \tag{5}$$

Segment ②:

$$x = L_1 + \rho_2 \sin \theta_2, \quad y = s_2, \quad z = \rho_2 \cos \theta_2; \quad y \ge L_1 - x, \quad s_2 \ge -\rho_2 \sin \theta_2. \tag{6}$$

   Expressions for the radius vectors of the pipe points follow from formulas (5), (6). Let's fix the numbering of curvilinear coordinates:

$$x_1 = s, \quad x_2 = \theta, \quad x_3 = \rho. \tag{7}$$

Next, we find the unit vectors of the basis of the curvilinear coordinate system using the formulas from the book [9]. The components of the metric tensor and the Lamé coefficients follow from these formulas:

$$g_{11}^{(i)} = 1, \quad g_{22}^{(i)} = \rho_i^2, \quad g_{33}^{(i)} = 1; \quad g^{11(i)} = 1, \quad g^{22(i)} = \frac{1}{\rho_i^2}, \quad g^{33(i)} = 1;$$

$$H_1^{(i)} = 1, \quad H_2^{(i)} = \rho_i, \quad H_3^{(i)} = 1; \quad i = 1, 2. \tag{8}$$

Formulas for the coefficients of the first quadratic form of the median surfaces $A^{(i)}$, $B^{(i)}$ and the curvatures of the median surfaces $k_1^{(i)}$, $k_2^{(i)}$ of cylindrical pipes follow from (8) for $\rho_i = R_0$:

$$A^{(i)} = 1, \quad B^{(i)} = R_0; \qquad k_1^{(i)} = 0, \quad k_2^{(i)} = R_0; \quad i = 1, 2. \tag{9}$$

In formulas (8), (9), the superscript indicates the segment number.

2.2. Equations of statics and dynamics

The dynamics of a pipeline is governed by the equations of an elastic body [9]:

$$\rho_t a^k = \triangledown_i \sigma^{ki}, \tag{10}$$

where ρ_t is the density of the pipe material, a^k are the acceleration components, σ^{ki} are the stress-tensor components, and $\triangledown_i$ is the covariant derivative.

In the stationary case, provided there are no external distributed loads, the equilibrium equations are:

$$\triangledown_i \sigma^{ki} = 0. \tag{11}$$

2.2.1. Mathematical model of the dynamics of a weakly bent pipeline

We use equations (10) to describe the limiting Case 1, that is, the dynamics of the slow motion of a weakly bent pipeline. Equations (11) are used to describe a pipeline with a kink under the action of internal pressure, that is, the limiting Case 2.

In Case 1, we make the assumption:

$$\lambda \ll 1. \tag{12}$$

For the study of the large-scale processes in Case 1, the movement of the inner flow is considered as quasi stationary. The Darcy's law of a friction [11] was chosen as the law of hydraulic resistance. The equations of stationary movement of an incompressible fluid are those of [11]:

$$\rho_f \left(\mathbf{v}_0, \nabla \right) \mathbf{v}_0 = -\nabla p - \mathbf{\Phi} \left(\vartheta_{s0} \right), \quad \left(\nabla, \mathbf{v}_0 \right) = 0, \quad \rho_f = \text{const.} \tag{13}$$

We denoted: ρ_f- fluid density inside the pipe, μ_f- fluid viscosity, p- fluid pressure. The components of the fluid velocity vector $\mathbf{v}_0$ along the coordinate axes s, θ, R are denoted as v_s, v_θ, v_R, respectively.

The resisting force $\mathbf{\Phi} \left(\vartheta_{s0} \right)$, affecting on a fluid stream was described in [11].

Under assumption (12), the system of equations was obtained [4]:

$$\frac{1}{A} \frac{\partial I^{(0)}}{\partial s} - \frac{1-v}{B} \frac{\partial \chi_0}{\partial \theta} + (1-v) \left(k_1 k_2 u - \frac{k_2}{A} \frac{\partial w}{\partial s} \right) = -\frac{1-v^2}{Eh} X,$$

$$\frac{1}{B} \frac{\partial I^{(0)}}{\partial \theta} + \frac{1-v}{A} \frac{\partial \chi_0}{\partial s} + (1-v) \left(k_1 k_2 v - \frac{k_1}{B} \frac{\partial w}{\partial \theta} \right) = -\frac{1-v^2}{Eh} Y,$$

$$-(k_1 + k_2) \cdot I^{(0)} + \frac{1-v}{AB} \left[2ABk_1 k_2 w + \frac{\partial}{\partial s} (Bk_2 u) + \frac{\partial}{\partial \theta} (Ak_1 v) \right] - \frac{h^2}{12} \nabla^2 \nabla^2 w -$$

$$- \frac{h^2}{12} \nabla^2 \left[\left(k_1^2 + k_2^2 \right) w \right] = -\frac{1-v^2}{Eh} Z; \tag{14}$$

$$\nabla^2 = \frac{1}{AB} \left[\frac{\partial}{\partial s} \left(\frac{B}{A} \cdot \frac{\partial \cdot}{\partial s} \right) + \frac{\partial}{\partial \theta} \left(\frac{A}{B} \cdot \frac{\partial \cdot}{\partial \theta} \right) \right].$$

$$I^{(0)} = \frac{1}{A}\left(\frac{\partial u}{\partial s} + \frac{A}{R_0}\frac{\partial v}{\partial \theta} + v\kappa\cos\theta\right) + \frac{1}{A}\left(\frac{A}{R_0} + \kappa\sin\theta\right)w - \frac{1}{2A^2}\left[\left(\frac{\partial w}{\partial s}\right)^2 + \left(\frac{\partial v}{\partial s}\right)^2\right],$$

$$\chi_0 = \frac{1}{2AB}\left[\frac{\partial}{\partial s}(Bv) - \frac{\partial}{\partial \theta}(Au)\right];$$

$$\frac{1}{h}X = -\rho_t\frac{\partial^2 u}{\partial t^2} + \frac{1}{h}\Phi_t(\vartheta_{s0}),$$

$$\frac{1}{h}Y = -\rho_t\frac{\partial^2 v}{\partial t^2} - \frac{2\mu u^* \cos\theta}{hR_0\left(0.5 - \ln\left|\frac{\gamma}{4}\frac{\rho_e u^*}{\mu}R_0\right|\right)},$$

$$\frac{1}{h}Z = -\rho_t\frac{\partial^2 w}{\partial t^2} + \frac{1}{h}(p - p_e).$$

Here is denoted: u, v, w – displacements of the median pipe surface along the coordinates s, θ, R; $I^{(0)}$, χ_0 – the first invariant of the strain tensor and the linear torsion of the pipe wall; X, Y, Z – the components of the forces density acting on the shell along the coordinates s, θ, R, respectively; p_e – external pressure. Functions A, B are defined by the formulas (2).

The system of equations (14) is supplemented by the boundary conditions of rigid fixing and by the homogeneous initial conditions:

$$u = 0, \quad v = 0, \quad w = 0, \quad \frac{\partial w}{\partial s} = 0 \text{ at } s = 0, \quad s = L \text{ and any } t;$$

$$u = 0, \quad v = 0, \quad w = 0; \quad \frac{\partial u}{\partial t} = 0, \quad \frac{\partial v}{\partial t} = 0, \quad \frac{\partial w}{\partial t} = 0 \text{ at } t = 0. \tag{15}$$

Equations (14) with boundary and initial conditions (15) are a complete three-dimensional mathematical model in Case 1.

2.2.2. Mathematical model of a pipeline with a singular profile

Above, we designated as Case 2 the situation when

$$\lambda \to \infty. \tag{16}$$

In this case, we restrict ourselves to studying the stationary equations (11). The action of the internal medium on the pipe is reduced to the inclusion of known pressure in the equilibrium equations of the shell.

The statement of the problem within the framework of the moment shells theory for case (16) was studied in detail in [5]. Based on the introduced coordinate systems (5)–(7) and parameters (8), (9), two systems of equations of a two-dimensional mathematical model were derived from equations for a solid body (11):

$$\frac{\partial^2 u_i}{\partial s_i^2} + \frac{1-v}{2R_0^2}\frac{\partial^2 u_i}{\partial \theta_i^2} + \frac{1+v}{2R_0}\frac{\partial^2 v_i}{\partial s_i\partial \theta_i} + \frac{v}{R_0}\frac{\partial w_i}{\partial s_i} - \frac{h^2}{12R_0}\frac{\partial^3 w_i}{\partial s_i^3} + \frac{(1-v)h^2}{24R_0^3}\frac{\partial^3 w_i}{\partial s_i\partial \theta_i^2} + \frac{1-v^2}{Eh}X_i = 0,$$

$$\frac{1+v}{2R_0}\frac{\partial^2 u_i}{\partial s_i\partial \theta_i} + \frac{1}{R_0^2}\frac{\partial^2 v_i}{\partial \theta_i^2} + \frac{1-v}{2}\frac{\partial^2 v_i}{\partial s_i^2} + \frac{1}{R_0^2}\frac{\partial w_i}{\partial \theta_i} - \frac{3-v}{2}\frac{h^2}{12R_0^2}\frac{\partial^3 w_i}{\partial \theta_i\partial s_i^2} + \frac{1-v^2}{Eh}Y_i = 0, \tag{17}$$

$$-v\frac{\partial u_i}{\partial s_i} - \frac{1}{R_0}\frac{\partial v_i}{\partial \theta_i} - \frac{w_i}{R_0} + \frac{h^2}{12}\left(\frac{\partial^3 u_i}{\partial s_i^3} - \frac{2}{R_0^3}\frac{\partial^2 w_i}{\partial \theta_i^2} + \frac{3-v}{2R_0}\frac{\partial^3 v_i}{\partial \theta_i \partial s_i^2} - \right.$$

$$\left. - \frac{1-v}{2R_0^2}\frac{\partial^3 u_i}{\partial s_i \partial \theta_i^2}\right) - \frac{h^2}{12}R_0\left(\frac{\partial^4 w_i}{\partial s_i^4} + \frac{2}{R_0^2}\frac{\partial^4 w_i}{\partial s_i^2 \partial \theta_i^2} + \frac{1}{R_0^4}\frac{\partial^4 w_i}{\partial \theta_i^4}\right) + R_0\frac{1-v^2}{Eh}Z_i = 0.$$

Here, X_i, Y_i, Z_i are the components of the surface external force acting on the shell; u_i, v_i, w_i are the components of the displacement vector of the middle surface of the i-th segment.

The boundary conditions number at each end of the bent shell is four, as shown in [12]. This condition can be rigidly fixed as in [4]:

$$
\begin{aligned}
u_1 = v_1 = w_1 = 0; &\quad \frac{\partial w_1}{\partial s_1} = 0, &\quad \text{for} \quad s_1 = 0; \\
u_2 = v_2 = w_2 = 0; &\quad \frac{\partial w_2}{\partial s_2} = 0, &\quad \text{for} \quad s_2 = L_2.
\end{aligned}
\tag{18}
$$

Next, we impose the conjugation conditions on the shell connection line to close the boundary value problem (17), (18). The formulas for the conjugation conditions were obtained in [5].

The geometric conditions at the contact are as follows:

$$v_2 - u_2\cos\theta = v_1 + u_1\cos\theta, \quad u_2 + v_2\cos\theta + w_2\sin\theta = u_1 - v_1\cos\theta - w_1\sin\theta,$$

$$- u_2\sin\theta - v_2\sin\theta\cos\theta + w_2\left(1 + \cos^2\theta\right) =$$
$$= u_1\sin\theta - v_1\sin\theta\cos\theta + w_1\left(1 + \cos^2\theta\right), \tag{19}$$

$$\frac{\partial w_1}{\partial\theta} = \frac{\partial w_2}{\partial\theta}.$$

Equalities (19) contain a complete set of geometric conjugation conditions on the connection line of the median surfaces of cylindrical pipes.

Pairing conditions for force factors:

$$M^{(1)} = M^{(2)}; \qquad S^{(1)} = -S^{(2)};$$
$$-Q^{(2)}\sqrt{1 + 3\cos^2\theta} + N^{(2)}\sin\theta = N^{(1)}\sin\theta + Q^{(1)}\sqrt{1 + 3\cos^2\theta}; \tag{20}$$
$$-Q^{(2)}\sin\theta - N^{(2)}\sqrt{1 + 3\cos^2\theta} = N^{(1)}\sqrt{1 + 3\cos^2\theta} - Q^{(1)}\sin\theta.$$

Here denoted: $M^{(i)}$ are bending moments, $S^{(i)}$ are shear forces, $Q^{(i)}$ are cutting efforts, $N^{(i)}$ are normal efforts, (i) stands for segment number. Expressions of force factors (20) through the wall displacements is given in [5].

The mathematical model of connected pipes as the moment shell consists of the components:

1. System of equations (17) with boundary conditions (18);
2. Geometric conditions on the connection line (19);
3. Interface conditions for power factors on the connection line (20).

3. Methods of computing experiments

3.1. Pipe bending problem

This section discusses a method for solving the problem of Case 1. In this case the condition (12) is satisfied. Let's introduce dimensionless variables in equations (14):

$\zeta = s/\ell$, $r = R/R_0$, $\theta = \theta$, $\tau = \omega t$. Here ℓ, ω are the characteristic length and frequency of processes in the pipeline.

The displacements of the pipe median surface in the dimensionless form are denoted by symbols: $u' = u/R_0$, $v' = v/R_0$, $w' = w/R_0$.

The dimensionless components of the fluid velocity: $v'_s = v_{s0}/\omega\ell$, $v'_\theta = v_{\theta0}/\omega\ell$, $v'_r = v_{R0}/\omega\ell$; pressure in the fluid: $p' = P/p_a$. The length of the pipe centerline in a dimensionless form: $L' = L/\ell$.

Let us bring equations (14) to dimensionless form. Then we represent their solutions in the form:

$$
\begin{aligned}
u'(\zeta, \theta, \tau) &= u_0(\zeta) + \lambda u_1(\zeta, \tau) \sin\theta + O\left(\lambda^2\right); \\
v'(\zeta, \theta, \tau) &= \lambda v_1(\zeta, \tau) \cos\theta + O\left(\lambda^2\right); \\
w'(\zeta, \theta, \tau) &= w_0(\zeta) + \lambda w_1(\zeta, \tau) \sin\theta + O\left(\lambda^2\right); \\
p'(\zeta, \theta, r) &= p^{(0)}(\zeta, r) + \lambda p^{(1)}(\zeta, r) \sin\theta + \lambda p^{(2)}(\zeta, r) \cos\theta + O\left(\lambda^2\right).
\end{aligned}
\tag{21}
$$

Within the framework of this work, the dynamics of the fluid is considered known; its study is available in [8, 4]. The zero-order solutions (21) are also assumed to be known.

The equations of the first approximation have the form (see [4]):

$$
\alpha^2 \frac{\partial^2 u_1}{\partial \zeta^2} - \frac{1-\nu}{2} u_1 - \frac{1+\nu}{2} \alpha \frac{\partial v_1}{\partial \zeta} + \nu\alpha \frac{\partial w_1}{\partial \zeta} +
$$

$$
+ f\left[\frac{1-\nu}{2} u_0 - 2\alpha^2 \frac{\partial^2 u_0}{\partial \zeta^2} + \alpha(1-\nu)\frac{\partial w_0}{\partial \zeta}\right] -
$$

$$
- \alpha^3 \left(\frac{\partial w_1}{\partial \zeta}\frac{\partial^2 w_0}{\partial \zeta^2} + \frac{\partial w_0}{\partial \zeta}\frac{\partial^2 w_1}{\partial \zeta^2}\right) + 3\alpha^3 f \cdot \frac{\partial w_0}{\partial \zeta}\frac{\partial^2 w_0}{\partial \zeta^2} = \frac{\rho_t R_0^2 \omega^2}{E^*} \frac{\partial^2 u_1}{\partial \tau^2};
\tag{22}
$$

$$
\frac{1-\nu}{2} \alpha^2 \frac{\partial^2 v_1}{\partial \zeta^2} - v_1 - \frac{1}{E^* h^*} \frac{2u_1^* \mu}{R_0 \left(0.5 - \ln\left|\frac{\gamma\rho_e \lambda u_1^*}{4\mu} R_0\right|\right)} + \frac{1+\nu}{2} \alpha \frac{\partial u_1}{\partial \zeta} +
$$

$$
+ w_1 + f\left(w_0 - \frac{3-\nu}{2}\alpha\frac{\partial u_0}{\partial \zeta}\right) - \alpha^2 \frac{\partial w_0}{\partial \zeta}\frac{\partial w_1}{\partial \zeta} = \frac{\rho_t R_0^2 \omega^2}{E^*}\frac{\partial^2 v_1}{\partial \tau^2};
\tag{23}
$$

$$
w_1 + \frac{h^{*2}}{12}\left(\alpha^4 \frac{\partial^4 w_1}{\partial \zeta^4} - \alpha^2 \frac{\partial^2 w_1}{\partial \zeta^2}\right) + \nu\alpha\frac{\partial u_1}{\partial \zeta} - v_1 +
$$

$$
+ f\left[2\nu w_0 + (1-\nu)\alpha\frac{\partial u_0}{\partial \zeta}\right] - \alpha^2 \frac{\partial w_0}{\partial \zeta}\frac{\partial w_1}{\partial \zeta} + \frac{\alpha^2}{2} f\left(\frac{\partial w_0}{\partial \zeta}\right)^2 =
$$

$$
= \frac{1}{E^* h^*}\left[\rho_f \vartheta_{s0}^2 f - \frac{2u_1^* \mu}{R_0\left(0.5 - \ln\left|\frac{\gamma\rho_e\lambda u_1^*}{4\mu} R_0\right|\right)}\right] - \frac{\rho_t R_0^2 \omega^2}{E^*}\frac{\partial^2 w_1}{\partial \tau^2}.
\tag{24}
$$

The boundary conditions for (22)–(24) can be easily obtained from (15), (21).

Thus, the three-dimensional problem (14), (15) is reduced to a one-dimensional formulation. A difference scheme for numerical solution of equations (22)–(24) was constructed in [4]. Ibid, the high accuracy of this scheme was proved.

The main geometric characteristic of the solution is the function:

$$
w_n = -\frac{\lambda R_0}{2}\left(v_1 + w_1\right).
$$

The physical meaning of this function is the pipe centerline displacement in its plane. Knowing the displacements of the pipe walls, it is easy to calculate the longitudinal ε_s and angular ω strains of its wall.

3.2. Numerical method for kinked pipe

In the kinked pipe problem, we have a connection line between pipes. Singularity points of the stress field appear in shells with such lines, as noted in [3]. The problem of calculating such a stress field is close in a mathematical sense to the problem of calculating stresses in an L -shaped domain, see [13]. Therefore, to solve the problem under condition (16), it is necessary to develop a new computational algorithm. We plan to create this algorithm based on the approach developed in [13, 14, 15, 16, 17, 18, 19].

In this work, the aim was set to illustrate the existence of a stress field singularity and to estimate the limiting stress values. This objective can be achieved by using existing software applications. Therefore, numerical experiments on calculating the stress-strain state of a pipeline with a break in the profile were performed in the FreeCAD software package. An overview of the software package is given in [20].

We have created a pipeline modeling algorithm in the FreeCAD software package. It provides for the creation of a solid 3D model, building a mesh of the finite element method, entering data, setting up the solver, setting up computational experiments, and visualizing the calculation results. The algorithm uses the CalculiX finite element method package and the NetGen meshing package.

4. Numerical results and discussion

4.1. Numerical investigation of the pipe bending problem

Here we investigate several problems under condition (12).

Several physical and geometrical parameters in all problems coincide and are equal: h = 0.005 m, ρ_e = 1700 kg$/$m^3, μ = 10000 N $\cdot$ s/m^2, ρ_t = 7200 kg$/$m^3, E = 2.07 $\cdot$ 10^{11} N/m^2, v = 0.24, R_0 = 0.3 m, μ_f = 0.667 N $\cdot$ s/m^2, and ρ_f = 850 kg$/$m^3. These parameters approximately correspond to a light oil stream in a steel pipe.

Problem 1. The pipe centerline is described by the fractional-rational function:

$$y = 40(1 - 0.001x) / \left(1 + 10^{-6}x^2\right), \quad -6000 \le x \le 6000.$$

The pipeline length: L = 12000 m. Uniform current velocity ϑ_{s0} = 1 m/s; calculated interval of time T_{end} = 691200 s.

Problem 2. The pipe centerline is described by the function (cubic parabola):

$$y = 10^{-8}x\,(x - 6000)\,(x - 12000), \quad 0 \le x \le 12000.$$

The pipeline length: L = 12500 m. Uniform current velocity ϑ_{s0} = 1 m/s; calculated over the interval of time T_{end} = 864000 s.

The following functions were found, as the numerical experiments results: displacements of the centerline $w_n\,(t, s)$, angular wall strains $\omega\,(s, \theta)$ at the time final moment $t = T_{end}$, and the coordinates of the centerline $x(t, s)$, $y(t, s)$.

From expressions (21) follows that the physical sense of $\lambda u_1 R_0$ is a displacement of points from the cross-sectional plane perpendicular to the pipe centerline, i.e. warping, see [6]. This fact is verified
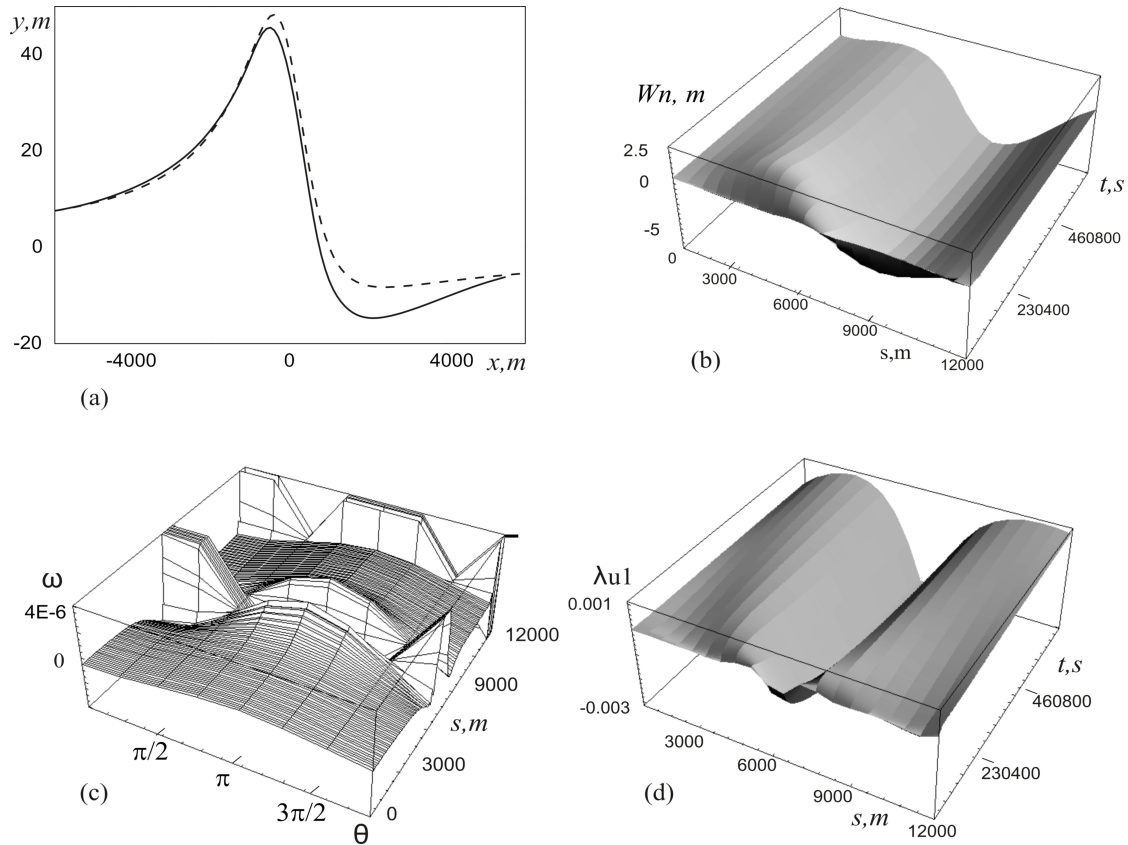
Figure 1: (a) – the coordinates of the profile at the start (dashed line) and at the end of the calculation; (b) – the displacement of the axial line; (c) – the angular strain of the pipe's wall, (d) – the longitudinal displacement in a first approximation.

by direct calculation with $u_1 = const$. Sectional warping of the cross-section of a cylindrical pipe was observed in the experiments of V.S. Vlasov [7]. Functions $u_1(t, s)$ were calculated, reflecting the magnitude of the cross sections warping.

Problem 1 solution.

For problem 1 coordinates and displacements of the pipe centerline shown in Figure 1 (a), (b) respectively. This illustrate the coherence of the numerical calculations for the offered mathematical model with the mechanical fundamental laws: the displacement of a profile is directed towards the distributed loading from a fluid flow.

In Figure 1 (c), (d) angular strain and the cross-sections warping in problem 1 are represented. The angular strains shown in Figure 1 (c) illustrate the cross-sections distortion in the wide vicinity and at the fixing points of the profile. The cross-sectional warping occurred in this problem, with a warping on the order of $0.003R_0$, see Figure 1 (d).

Problem 2 solution.

The coordinates of a profile of the pipeline and its warping of cross-sections in problem 2 represented in Figure 2 (a), (b), respectively. Similar to problem 1, the change in the coordinates of the profile at the start (dotted line) and at the end of the calculation in Figure 2 (a) indicates the numerical experiment coherence with the mechanics laws. This numerical experiment indicated the existence of the cross-sectional warping of the long thin-walled pipeline of the order $0.02R_0$ as shown in Fig-
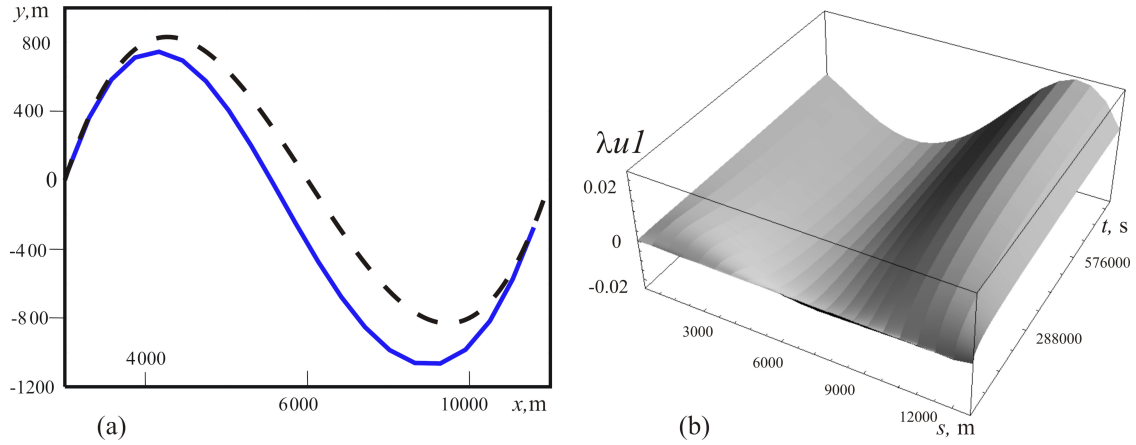
Figure 2: (a) – the coordinates of the profile at the start (dashed line) and at the end (blue line) of the calculation; (b) – the longitudinal displacement in a first approximation (warping).

ure 2 (b).

Thus, in this section the problem about reaching of equilibrium position of a pipe for two types of the pipeline profile was solved numerically. The coherence of the numerical calculations for the offered mathematical model with the mechanical fundamental laws were illustrated. The angular strains were calculated; this parameter illustrate the cross-sections distortion in the wide vicinity and at the fixing points of the profile. The existence of the pipe cross-sections warping was proved. Angular strains of the pipeline's wall are calculated when the pipe reaches a state of equilibrium. It is found that the irregular strains occur in the vicinity of the pinning points or extreme camber.

4.2. Numerical investigation of the problem of a pipeline with a kink

Here we investigate several problems under condition (16). Problems were solved for two pipes of the same material and with similar geometry, but these pipes were subjected to different loads.

To numerically illustrate the presence of a singularity in the solution, the free software package FreeCAD (see [20]) with the built-in program for calculating the finite element method CalculiX was used. These software packages allow us to see the growth of stresses in the vicinity of the joint line.

FreeCAD was first tested using the Lamé problem for a thick-walled pipe under internal pressure. The exact solution to this problem is given in [9]. The test calculation showed agreement between the approximate solution obtained by FreeCAD and the exact solution.

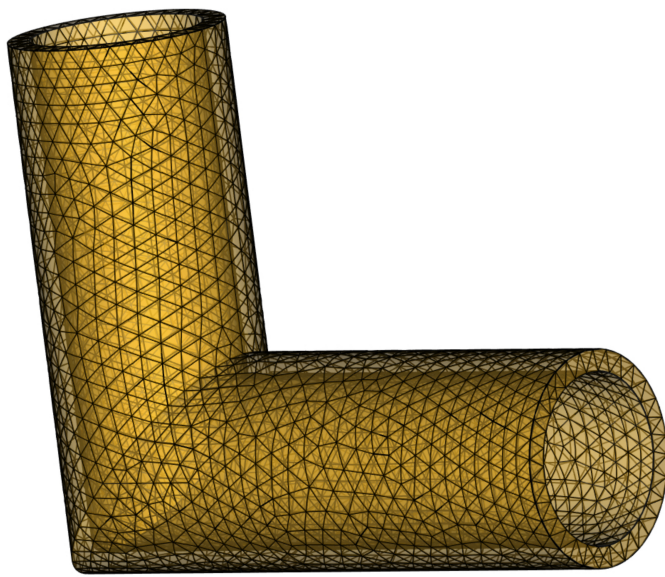The geometry of all problems was described in subsection 2.1.2.

Problem 1. Geometric parameters: h = 20 mm, R_0 = 90 mm, L_1 = 500 mm, L_2 = 400 mm. Material: S335JO steel, material parameters: ρ_t = 7800 kg/m^3, E = 210 GPa, ν = 0.3, σ_t = 343 MPa, $[\sigma_B]$ = 490 MPa.
Rigid constraints were specified on the outer ends of the pipes; this corresponds to boundary conditions (18). A uniformly distributed pressure was imposed on the entire inner surface of the pipes with a value of p = 100 MPa.
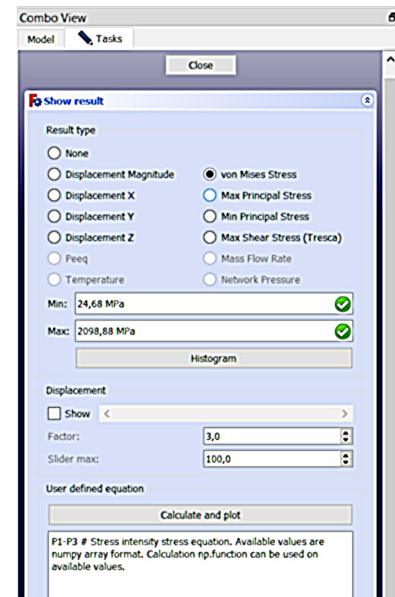
Problem 2. Geometric parameters: h = 5 mm, R_0 = 47.5 mm, L_1 = 250 mm, L_2 = 250 mm. Material: S335JO steel.
Rigid constraints were specified on the outer ends of the pipes. A uniformly distributed pressure was imposed on the entire inner surface of the pipes with a value of p = 10 MPa.

Problem 1 solution.

Figure 3: Problem 1: FEM mesh and von Mises stress.

The mesh generated by the NetGen mesh generator built into FreeCAD and the von Mises stress limits are shown in Figure 3. In Figure 3 (a) you can see a slight thickening of the mesh in the vicinity of the pipe joint line. This is caused by setting the precision as average when generating the mesh.

In Figure 3 (b) you can see a significant variation in von Mises stresses between maximum and minimum stresses. This illustrates that stresses have domains of rapid growth, in other words, the stress field has singularities. The maximum stress reaches 2098 MPa, which significantly exceeds the ultimate strength of S335JO steel. This value is achieved on the inner side of the pipe wall in the reentrant corner of the domain at $\theta = 3\pi/2$, at the joint line, only at a few nodes of the FEM grid. However, the stress drops to 25 MPa at the nodes of the FEM grid located far from the pipe connection line.

Problem 2 solution.

The mathematical model of the finite element method for Problem 2 was built in the FreeCAD software package. FEM mesh parameters: number of nodes equal 31514, number of element surfaces equal 10526, number of volume elements equal 15651. Mesh parameters have been set to high precision. As a result of calculations by the finite element method, the stress distribution was found, see Figure 4.

In Figure 4 (a) shows the stress gradient from maximum red to minimum green. In Figure 4 (b) shows a histogram of stress distribution by the number of grid nodes. Limiting stress values in Problem 2: the maximum stress is 395.5 MPa, the average stress is 89.5 MPa, the minimum stress is 2.9 MPa.

So, let's summarize the results of the paragraph. An algorithm for mathematical modeling of the pipeline in the FreeCAD software package has been created. The stress fields were found by the finite element method, and the corresponding results were presented and visualized. Differences in the solutions of problems 1, 2 are caused by the difference in the loading data and the difference in geometric parameters. But these differences are not fundamental.

The main thing in the results obtained is the presence of a singularity in the stress field. When comparing the numerical solutions of problems 1, 2 with the numerical solution of a mathematically
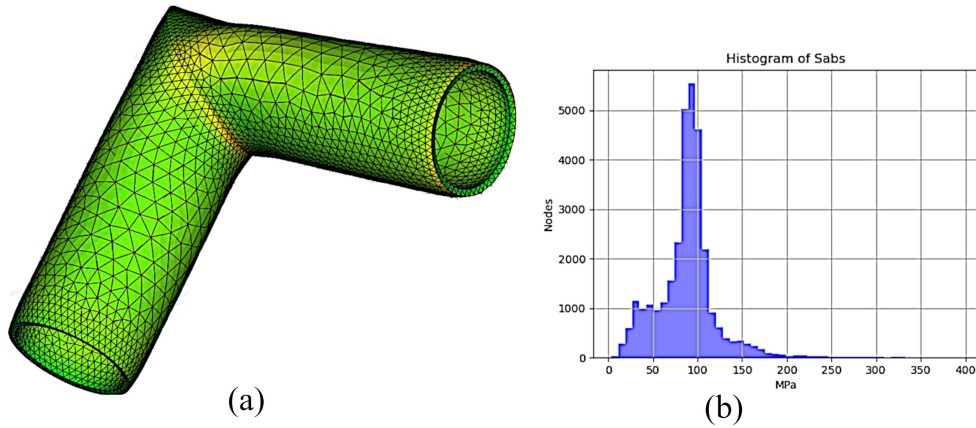
Figure 4: Problem 2. Stress field in the pipe: (a) – graphic isolines on FEM mesh; (b) – histogram.

close problem of the elasticity theory with an reentrant angle, considered in [21], we can conclude that these solutions are close in a qualitative sense.

5. Conclusion

A numerical criterion is determined that allows one to differentiate between two limiting states of the pipeline geometry. Two new mathematical models of the pipeline for each of these limits are presented: model (13), (14) for calculating the dynamics of a smoothly bent pipe; model (17)–(20) for calculating the stress-strain state of a pipeline with a singularity. Methods for the approximate solution of boundary value problems for the constructed mathematical models are proposed. For model (13), (14), a new algorithm for the reduction of a three-dimensional problem to its one-dimensional analog is proposed.

Numerical experiments have been performed. It was established that the proposed reduction algorithm for Case 1 yields results consistent with the data of other researchers. It was established that in Case 1, the cross section warping occur in the pipe.

In Case 2, the presence of a stress singularity on the pipe junction line was established. The calculation was performed by the finite element method in the FreeCAD design environment.

Acknowledgments

References

[1] I. Towhata, Geotechnical Earthquake Engineering, Springer-Verlag, Berlin, Heidelberg, 2008.

[2] M. Hamada (Ed.), Critical Urban Infrastructure Handbook, CRC Press, Taylor & Francis Group, London, New York, 2014.

[3] A. L. Gol'denveizer, Theory of Elastic Thin Shells, Published for the American Society of Mechanical Engineers by Pergamon Press, 1961.

[4] V. A. Rukavishnikov, O. P. Tkachenko, Dynamics of a fluid-filled curvilinear pipeline, Applied Mathematics and Mechanics 39 (2018) 905–922. doi:10.1007/s10483-018-2338-9.

[5] V. A. Rukavishnikov, O. P. Tkachenko, Mathematical model of the pipeline with angular joint of elements, Mathematical Methods in the Applied Sciences 43 (2020) 7550–7568. doi:10.1002/mma.5751.

[6] V. I. Samul, Fundamentals of the Elasticity and Plasticity Theory, High School, Moscow, 1982. (in Russian).

[7] V. S. Vlasov, Basic Differential Equations in General Theory of Elastic Shells, Technical Report NACA-TM-1241, National Advisory Committee for Aeronautics, Washington, 1951. URL: https://ntrs.nasa.gov/search.jsp?R=20050028489.

[8] V. A. Rukavishnikov, O. P. Tkachenko, Numerical and asymptotic solution of the equations of propagation of hydroelastic vibrations in a curved pipe, Journal of Applied Mechanics and Technical Physics 41 (2000) 1102–1110. doi:10.1023/A:1026619009228.

[9] L. I. Sedov, Mechanics of Continuous Media, World Scientific Publishing Company, Singapore, 1997.

[10] I. N. Bronstein, K. A. Semendyayev, A Guide Book to Mathematics: Fundamental Formulas, Tables, Graphs, Methods, Verlag Harri Deutsch, Springer-Verlag, Zürich, Frankfurt/Main, New York, 1973. doi:10.1007/978-1-4684-6288-3.

[11] L. G. Loitsyanskii, Mechanics of Liquids and Gases, Pergamon Press, Oxford-New York, 1966.

[12] V. V. Novozhilov, J. R. M. Radok, Thin Shell Theory (Paperback, Softcover reprint of the original 1st ed. 1964), Springer, Netherlands, 2014.

[13] V. A. Rukavishnikov, S. G. Nikolaev, On the R_ν-generalized solution of the Lamé system with corner singularity, Doklady Mathematics 92 (2015) 421–423. doi:10.1134/S1064562415040080.

[14] V. A. Rukavishnikov, On the existence and uniqueness of an R_ν-generalized solution of a boundary value problem with uncoordinated degeneration of the input data, Doklady Mathematics 90 (2014) 562–564. doi:10.1134/S1064562414060155.

[15] V. A. Rukavishnikov, E. V. Kuznetsova, The R_ν-generalized solution of a boundary value problem with a singularity belongs to the space $W_{2,\nu+\beta/2+k+1}^{k+2}(\Omega, \delta)$, Differential Equations 45 (2009) 913–917. doi:10.1134/S0012266109060147.

[16] V. A. Rukavishnikov, A. Y. Bespalov, An exponential rate of convergence of the finite element method for the Dirichlet problem with a singularity of the solution, Doklady Mathematics 62 (2000) 266–270.

[17] V. A. Rukavishnikov, E. V. Kuznetsova, A finite element method scheme for boundary value problems with noncoordinated degeneration of input data, Numerical Analysis and Applications 2 (2009) 250–259. doi:10.1134/S1995423909030069.

[18] V. A. Rukavishnikov, E. I. Rukavishnikova, Numerical method for Dirichlet problem with degeneration of the solution on the entire boundary, Symmetry 11 (2019) 1455. doi:10.3390/sym11121455.

[19] V. A. Rukavishnikov, A. O. Mosolapov, E. I. Rukavishnikova, Weighted finite element method for elasticity problem with a crack, Computers and Structures 243 (2021) 106400. doi:10.1016/j.compstruc.2020.106400.

[20] B. Collette, FreeCAD for Inventors: Practical Examples and Clear Descriptions, Purple Squirrel Productions LLC, 2018.

[21] V. A. Rukavishnikov, A. O. Mosolapov, Weigthed vector finite element method and its applications, Computer Research and Modeling 11 (2019) 71–86. doi:10.20537/2076-7633-2019-11-1-71-86.